Finite element modeling of the elastic-viscoplastic behavior of PC/ABS 60:40 blend under uniaxial compression

P.G. Marques Flávio[1], T. Doca[1], F.M. Andrade Pires[2], F. Macedo [2]

[1]*Department of Mechanical Engineering, University of Brasília*
ENM - Department of Mechanical Engineering, Faculty of Technology, University of Brasilia: Campus Darcy Ribeiro, 70910-900, Brasilia, DF, Brazil
paulo.guilherme@aluno.unb.br, doca@unb.br
[2]*DEMEC - Department of Mechanical Engineering, Faculty of Engineering, University of Porto: Rua Dr. Roberto Frias, 4200-465, Porto, Portugal*
fpires@fe.up.pt, fmacedo@fe.up.pt

Abstract. Nowadays the use of polymers presents itself as a viable alternative to replace parts and components that once were composed only of metallic and/or ceramic materials. The advancement of material engineering has enabled the creation of polymeric compounds with high resistance, but with a low density, which can be an advantage when compared to a wide range of various other materials. Along with the advances in obtaining new polymers, there was also an evolution of numerical models that describe the mechanical behavior of these materials. The numerical formulations previously used for metallic materials have failed to represent them effectively. Polymeric materials are highly dependent on several factors, among them the strain rate, working temperature and manufacturing process are configured as those of greatest relevance in the influence of the mechanical properties. Therefore, it is extremely important to use constitutive equations that consider the aforementioned nonlinear effects. The main objective of the present work is to model the mechanical behavior of the uniaxial compression test of PC/ABS 60:40 blends. For this purpose, the numerical models used to describe the elastic-viscoplastic behavior of the material are based on the works presented by Arruda, Mulliken and Boyce and were implemented as finite element explicit formulation within VUMAT subroutines using the commercial software Abaqus.

Keywords: PC/ABS 60:40, Mulliken-Boyce, Numerical Implementantion

1 Introduction

Currently, polymers present themselves as a viable alternative for the replacement of parts or components that once were composed only of metallic and/or ceramic materials, this trend aims to improve tribological characteristics and reduce costs. Manufacture advancement in conjunction with the evolution of material engineering has enabled polymers of greater strength, lower density and lower cost to be obtained. According to Billemeyer [1], the mechanical properties of polymers can be defined from the response of this material under the application of external loads. The nature of this response depends on several factors intrinsic to the polymer manufacturing process, such as temperature, processing time and conditions, polymerization process controls, among others. Not least, the test conditions also have a great influence on the response of the material, such as: test temperature, loading/unloading time and strain rate.

The polymer has a versatile profile, being part of the composition from packaging materials to highly complex structures, such as the Boing Dreamliner aircraft, where 50 % its entire structure is composed of polymeric materials. According to research carried out by Word Economy Forum [2], the grow in polymer production increased from 15 million tons in 1964 to 311 million tons in 2014. In parallel to the growing use of polymers for the most diverse purposes, there has also been advancement in numerical methods capable of predicting the mechanical behavior of these materials, since the methods applicable to metals are unable to represent their behavior in a striking way.

Acrylonitrile Butadiene Styrene (ABS) is a lightweight and rigid polymer, obtained by the polymerization of styrene and acrylonitrile in the presence of polybutadiene, presenting resistance to impact and flexibility. Polycarbonate (PC) is a durable material that has high tensile strength, impact resistance and flame resistance.

PC/ABS (Polycarbonate / Acrylonitrile - Butadiene-Styrene) is a mixture of PC and ABS, which provides a combination of the high processability of ABS with the excellent mechanical properties, thermal resistance and impact of PC. PC/ABS blends provide excellent resistance to impact at low temperatures which is better than that presented by ABS or PC, which provides a wide application in the electronics industry and the automotive industry. This material has high impact resistance, thermal resistance, high rigidity, good processability and high dimensional precision.

Because polymeric materials have a greater diversity of mechanical behavior, commonly each numerical method is valid for a restricted range of polymers. Among the various numerical models present in the bibliography, we can mention Ogden model (Ogden [3]), Suchoki (Suchocki [4]), Bergstrom-Boyce (J.S. Bergström [5]), Arruda-Boyce (E.M. Arruda [6]), Hybrid model (J.S. Bergström [7]) and Mulliken-Boyce (A.D. Mulliken [8]).

In view of the points exposed so far, the main objective of the present work is to model the mechanical behavior of the PC/ABS 60:40 in a uniaxial compression test. Therefore, the Mulliken-Boyce numerical model in an explicit numerical integration environment through VUMAT's in the commercial software ABAQUS is implemented. Calibrations with the experimental test were used for the definition of the basic properties of the model.

2   Constitutive Modeling

The Mulliken-Boyce numerical model presents itself as an evolution of the model presented by E.M. Arruda [6]. In this model, instead of using a viscoplastic network, there are two networks in parallel called activated molecular processes, each with their respective elastic and viscoplastic properties, as represented in the figure 1.

The basic principle present in the viscoplastic behavior of the material is based on the flow theory of Ree-Eyring, where, there is the presence of several active processes that can contribute to the general behavior of the material. Physically, such processes can be understood as movements at molecular levels, presenting a threshold, determined by temperature and deformation rate, below which the associated molecular movement is restricted. Such a restriction can be understood as the general resistance to deformation of the material.
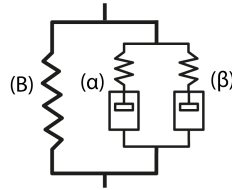

Figure 1: One-dimensional rheological representation of the Mulliken-Boyce model.

The intermolecular contribution to the stress state of the alpha and beta chains is obtained by deformation of the material through the constitutive laws of springs in a linear-elastic domain, as shown below. It is noteworthy that the real tensions are obtained from Hencky's hyperelastic behavior.

$$\boldsymbol{T}_{A,\alpha} = \tfrac{1}{J_\alpha} \mathcal{L}_\alpha^e [ln(\boldsymbol{U}_{A,\alpha}^e)]$$

$$\boldsymbol{T}_{A,\beta} = \tfrac{1}{J_\beta} \mathcal{L}_\beta^e [ln(\boldsymbol{U}_{A,\beta}^e)] \tag{1}$$

Since the constitutive model is represented by two viscoplastic components in parallel with a non-linear entropic hardening component, referring to the $BackStress$, it is possible to show that, under the application of any load, all components are subjected to the same deformation, therefore:

$$\boldsymbol{F}_{A,\alpha} = \boldsymbol{F}_{A,\beta} = \boldsymbol{F}_B = \boldsymbol{F} \tag{2}$$

Where, the $\boldsymbol{F}_{A,\alpha}$ and $\boldsymbol{F}_{A,\beta}$ contribution can be determined by the following equations:

$$\boldsymbol{F}_{A,\alpha} = \boldsymbol{F}^e_{A,\alpha} \boldsymbol{F}^p_{A,\alpha}$$

$$\boldsymbol{F}_{A,\beta} = \boldsymbol{F}^e_{A,\beta} \boldsymbol{F}^p_{A,\beta}$$

(3)

The conduction stresses $\boldsymbol{N}_\alpha$ and $\boldsymbol{N}_\beta$ are used to specify the directions of the tensors $\boldsymbol{F}^p_{A,\alpha}$, $\boldsymbol{F}^e_{A,\beta}$ and of the plastic flow, as presented in the equation 4. $\boldsymbol{T}'_{A,\alpha}$ and $\boldsymbol{T}'_{A,\beta}$ represent the deviatoric part of $\boldsymbol{T}_{A,\alpha}$ and $\boldsymbol{T}_{A,\beta}$, respectively.

$$\boldsymbol{N}_\alpha = \tfrac{1}{\sqrt{2}\tau_\alpha} \boldsymbol{T}'_{A,\alpha}$$

$$\boldsymbol{N}_\beta = \tfrac{1}{\sqrt{2}\tau_\beta} \boldsymbol{T}'_{A,\beta}$$

(4)

The equivalent effective shear stress (τ) is given by:

$$\tau_\alpha = \sqrt{\tfrac{1}{2}(\boldsymbol{T}'_{A,\alpha} : \boldsymbol{T}'_{A,\alpha})}$$

$$\tau_\beta = \sqrt{\tfrac{1}{2}(\boldsymbol{T}'_{A,\beta} : \boldsymbol{T}'_{A,\beta})}$$

(5)

Finally, the two constitutive laws for viscoplastic behavior alpha and beta ($\dot{\gamma}^p_\alpha$ and $\dot{\gamma}^p_\beta$) are described as:

$$\dot{\gamma}^p_\alpha = \dot{\gamma}^p_{0,\alpha} exp\left[-\tfrac{\Delta G_\alpha}{k\theta}\left(1 - \tfrac{\tau_\alpha}{s_{\alpha+\alpha_{p,\alpha}p}}\right)\right]$$

$$\dot{\gamma}^p_\beta = \dot{\gamma}^p_{0,\beta} exp\left[-\tfrac{\Delta G_\beta}{k\theta}\left(1 - \tfrac{\tau_\beta}{s_{\beta+\alpha_{p,\beta}p}}\right)\right]$$

(6)

In the equation 6, $\dot{\gamma}^p_\alpha$ and $\dot{\gamma}^p_\beta$ represent the pre-exponential factors, ΔG_α e ΔG_β the activation energy, p the pressure; $\alpha_{p,\alpha}$ and $\alpha_{p,\beta}$ the pressure coefficient. The internal variable s_α and s_β describes the athermic shear strength related to the shear modulus and respects the relationships presented below, where h_α and h_β represents the softening slope and s_{ss} is called the preferred state.

$$s_{0,\alpha} \equiv \tfrac{0,077\mu_\alpha}{1-\nu_\alpha}$$

$$\dot{s}_\alpha = h_\alpha\left(1 - \tfrac{s_\alpha}{s_{ss}}\right)\dot{\gamma}^p_\alpha$$

$$s_{0,\beta} \equiv \tfrac{0,077\mu_\beta}{1-\nu_\beta}$$

$$\dot{s}_\beta = h_\beta\left(1 - \tfrac{s_\beta}{s_{ss}}\right)\dot{\gamma}^p_\beta$$

(7)

In the Mulliken-Boyce model, the nonlinear hardening stress component (Backstress) due to the entropic resistance of the molecular alignment is defined as:

$$\boldsymbol{T}_B = \frac{C_R}{3}\frac{\sqrt{N}}{\lambda^p_{chain}}\mathcal{L}^{-1}\left(\frac{\lambda^p_{chain}}{\sqrt{N}}\right)\boldsymbol{B}^*_{dev}$$

(8)

Where, λ_{chain}^{p} presents the elongation in the network of eight chains and $\boldsymbol{B^*}_{dev}$ is the deviatory part of the left Cauchy-Green tensor. Finally, the total stress in the polymer is given by the tensorial sum of the contributions of the intermolecular stresses alpha and beta and the nonlinear hardening stress (BackStress):

$$\boldsymbol{T} = \boldsymbol{T_B} + \boldsymbol{T_{A,\alpha}} + \boldsymbol{T_{A,\beta}} \tag{9}$$

The Arruda-Boyce model, as well as the model presented by Mulliken-Boyce, can also be represented by a one-dimensional rheological model, however, unlike the Mulliken-Boyce model, it presents a single viscoplasticity network. When evaluating the contribution of nonlinear hardening, it appears that both models have similar equations, the main difference is that Mulliken-Boyce's model works with the total deformation gradient, whereas the Arruda Boyce model works with the plastic deformations gradient. As for the contribution of viscoplasticity, the main difference between the models lies in the fact that the Arruda-Boyce model is based on the equations presented by Argon and the Mulliken Boyce model on the Ree-Eyring theory. Equations 10 and 11 represent the contribution of nonlinear hardening and the intermolecular contribution to the Arruda-Boyce model, where, A represents the zero stress level activation energy.

$$\boldsymbol{T_B} = \frac{C_r}{\lambda_{chain}^{p}} \frac{\mathcal{L}^{-1}(\lambda_{chain}^{p}/N)}{\mathcal{L}^{-1}(1/N)} \boldsymbol{B^p}_{dev} \tag{10}$$

$$\dot{\gamma}^p = \dot{\gamma}^0 exp\left[-\frac{As}{k\theta}\left(1-\left(\frac{\tau}{s}\right)^{(5/6)}\right)\right] \tag{11}$$

Using the decomposition of the deformation gradient, the Cauchy stress can be calculated from the linear elastic relationship:

$$\boldsymbol{T} = \frac{1}{J^e}\mathcal{L}^e[ln(\boldsymbol{U^e})] \tag{12}$$

3 Methodology

To establish the parameters of the numerical model referring to the PC/ABS 60:40, the strategy was based on the adequacy of the curve obtained via Abaqus in reference to the experimental tests of the specimen's compression.

The compression tests were conducted following the ASTM D695–15 standard on a universal testing machine MTS 810 with a maximum capacity of 100 kN, where cylindrical test specimens of 9 mm in diameter and height were compressed to a total displacement of 6.1 mm at a deformation rate of 0.01 mm/s.

3.1 Material

As above-mentioned, the evaluated PC/ABS blend has 60% PC and 40% ABS in its composition, enabling the obtainment of a material with a mixture of properties of PC and ABS. Table 1 shows the main mechanical properties for PC, ABS and PC/ABS 60:40.

Table 1: Main mechanical properties: PC, ABS PC/ABS.

Properties	PC	ABS	PC/ABS 60:40
Density (kg/m^3)	1190	1040	1140
Tensile Modulus, 1.3 mm/min (MPa)	2340	2300	2340
Yield Stress, 50 mm/min (MPa)	62	44	54
Yield Strain, 50 mm/min (%)	7	2.2	4.5
Nominal Strain at break, 50 mm/min (%)	110	12	100

3.2   Numerical Model

The numerical modelling of the uniaxial compression test consists of a 1/4 cylinder with simetry conditions, as shown in figure 2(a) with an explicit time integration. In order to reproduce the contact between the upper and lower face of the specimen with the compression plates, a surface-to-surface interaction between the faces in contact was adopted. For the properties of the contact formulation, the penalty method was adopted for normal and tangential behavior, allowing contact separation for the first behavior mentioned and definition of a friction coefficient of 0.1 for the second.

Regarding the definition of contact, it is worth mentioning that the two support surfaces were represented as rigid bodies, in order to have a lower computational cost. The adoption of this numerical representation was based on the convergence of the simulation, as it allowed the convergence of the numerical tests for deformations greater than 50 %. The use of boundary conditions by displacement and rotation restrictions were previously used, however, the simulation conducted was not shown to be a viable alternative, since they presented great distortions in the elements of the restricted surfaces, thus causing failure of convergence.

The analysis of uniaxial compression of the cylindrical specimen was implemented from a structured mesh consisting solely of explicit hexagonal elements with an average dimension of $6.92 \times 10^{-4}\,m$, length obtained after conducting a study mesh convergence. Due to the presence of large deformations in the analyzes carried out, the use of distortion control and full integration was defined. The mesh adopted in the numerical model is shown in figure 2(b).

Two other important aspects for the implementation of the adopted model are the use of a non-linear increment of displacement, in order to impose on the simulation a constant deformation rate in time and use of the mass scaling tool for simulations since the dynamic effects have little relevance in the behavior of the analyzed object. This tool works in controlling the time step, especially in the small elements that end up controlling the simulation time increment.

In addition to the symmetry boundary conditions applied to the cylinder faces, as previously discussed, a encastre condition was applied to the lower plate, that is, restriction of all displacements and rotations. For the upper plate, all movements and rotations were restricted, except the displacements on the longitudinal axis, in order to allow compression of the specimen.

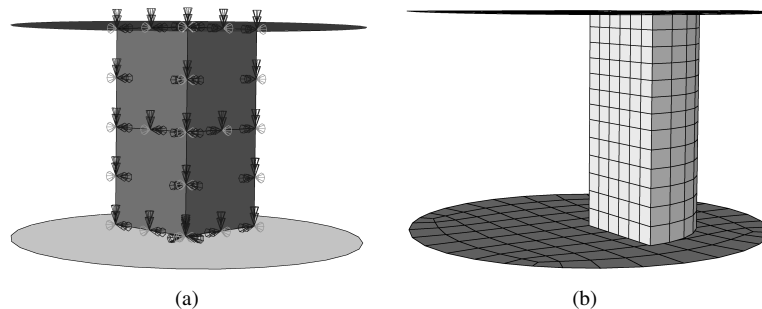(a)   (b)

Figure 2: FEM model of the cylindrical specimen employed for the the simulation of the uniaxial compression test: a) Boundary and symmetry conditions; b) representation of the four-noded haxahedra structural FE's used for cylindrical billet and the shell elements used for the loading application.

The numerical model was adopted to predict the behavior of the specimen up to 60 % axial strain rates, although it was able to predict at levels of strain of 100 %. For the complete simulation of the test specimen compression test, the simulation time was 113 seconds, in order to respect the strain rate imposed in the experimental test. The implementation of the Mulliken-Boyce model presented less convergence difficulties than the Arruda-Boyce model. For the first model, the time increment was in the order of 2.05×10^{-5} s, whereas for the Arruda-Boyce model the increase was 2.20×10^{-5} s, however, due to the greater complexity of the model Mulliken-Boyce, this model has a computational cost of approximately 57% higher. In both models, the time increment decreased as the magnitude of strain increased by approximately 42%.

4   Results

The behavior of the cylindrical specimen under the effect of uniaxial compression is represented in figure 3 in four different compression stages. The numerical model was adopted to predict the behavior of the specimen up to 60 % axial strain rates, although it was able to predict at levels of strain of 100 %.
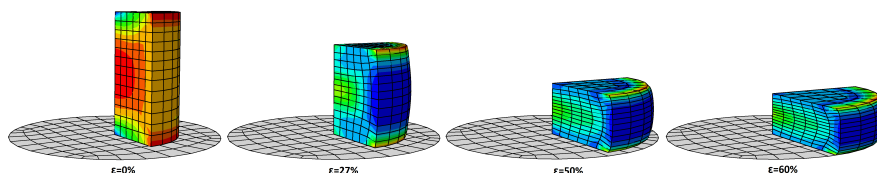
Figure 3: Representation of four stages of the uniaxial compression test simulation.

Figure 4 presents the comparative graphs between the experimental and numerical evaluations. It is possible to identify that both models showed a good prediction for the behavior of PC / ABS 60:40, as can be identified. When evaluating the linear elasticity zone, it appears that both numerical models presented identical predictions. The Mulliken-Boyce model showed the best fit in all other regions, with lesser fit in the transition phase between the linear elasticity zone and the beginning of the yield region. The Arruda-Boyce model showed a similar behavior to the Mulliken-Boyce model for the signaled transition region, however the behavior of the non-linear hardening region showed worse adequacy, as it increased more intensively than that verified experimentally.
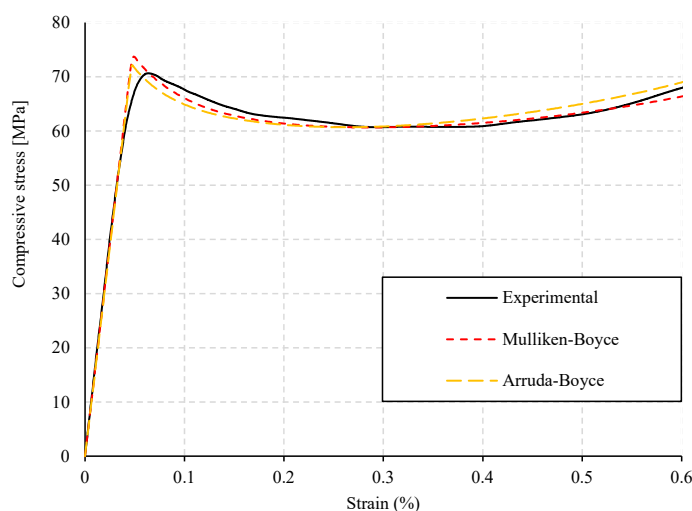

Figure 4: Uniaxial compression behavior of the PC/ABS 60:40: experimental data versus numerical models.

The most evident difference between the numerical representation of the non-linear hardening between the Mulliken-Boyce model and the Arruda-Boyce model is in the fact that in the second model, the non-linear hardening starts only after the occurrence of inelastic deformations, since its formulation is represented from the gradient of plastic deformation, this means that in the region of non-linear elasticity there is no hardening contribution of the polymer. In the Mulliken-Boyce model, as can be seen from the formulations presented above, the contribution of non-linear hardening occurs throughout whole the deformation, since the formulation is based on the total deformation gradient. In both models, the behavior of viscoplastic networks shows similar behaviors.

The main numerical parameters of the Arruda-Boyce model determined by the calibrations for the PC/ABS 60:40 modeling are shown in Table 2. Table 3 shows the main parameters of the Mulliken-Boyce model.

Table 2: Main Parameters: PC/ABS 60:40 - Arruda-Boyce Model.

Parameter	Value
Pre-exponential factor, ($\dot{\gamma}^p$)	$2.0 \times 10^{15} \ s^{-1}$
Zero Stress Level Activation Energy, (A)	$4.61 \times 10^{-17} m^3$
Softening slope, (h)	$500 \ MPa$
Preferred state, (s_{ss})	0.78
Ruberry modulus, (C_r)	$7.20 \ MPa$
Limiting chain extensibility, (N)	6.29

Table 3: Main Parameters: PC/ABS 60:40 - Mulliken-Boyce Model.

Parameter	Value
Pre-exponential factor, α ($\dot{\gamma}^p_{0,\alpha}$)	$2.98 \times 10^{16}\ s^{-1}$
Pre-exponential factor, β ($\dot{\gamma}^p_{0,\beta}$)	$3.39 \times 10^5\ s^{-1}$
Pressure coefficient, α ($\alpha_{p,\alpha}$)	0.168
Pressure coefficient, β ($\alpha_{p,\beta}$)	0.245
Activation energy, α (ΔG_α)	$4.10 \times 10^{-19} J$
Activation energy, β (ΔG_β)	$3.77 \times 10^{-20} J$
Softening slope, (h_α)	$350\ MPa$
Preferred state, (s_{ss})	0.73
Ruberry modulus, (C_r)	$8.20\ MPa$
Limiting chain extensibility, (N)	5.29

5   Conclusions

In view of the results presented, it is possible to verify that both the Arruda-Boyce model and the Mulliken-Boyce model, models developed for the evaluation of PC and PPMA (Polymethyl methacrylate), presented themselves as viable alternatives for the numerical representation of the mechanical behavior of PC/ABS 60:40 for the strain levels imposed in the presented study. The study conducted for the evaluation of a uniaxial compression showed good correlations with the results obtained experimentally, where the Arruda-boyce model presented a determination coefficient of 0.977 and the Mulliken-Boyce model a coefficient of 0.986. While the Arruda-Boyce model has a lower computational cost for numerical implementation due to the presence of a single elasto-viscoplastic network, the Mulliken-Boyce model presents better simulation convergence. For higher deformation levels (deformations above 60%), the Mulliken-Boyce model presents itself as the most viable alternative.

When evaluating the correlation between all numerical curves, it is possible to identify that the region with the greatest divergence between the numerical and experimental results is related to the zone of beginning of yield, more precisely after the region of linear elasticity.In this region, the biggest percentage difference between the experimental and numerical results was 14.08% for the Mulliken-Boyce model and 15.59% for the Arruda-boyce model, due to the numerical models showing an enlargement of the region of linear elasticity . For the other zones, that is, the region of yield and non-linear hardening, the biggest percentage error of the Mulliken-Boyce model was 2.58% and that of Arruda-Boyce was 4.27%. The Mulliken-Boyce presents an alternative for a better fit between the curves with a more accurate calibration of the beta chain or the use of some alternative as statistical resources, in order to allow a smoother transition between the end of the linear elasticity zone and the beginning of the polymer's yield. Another viable alternative is to apply new representations of the visco-plastic chains.

References

[1] Billemeyer, F., 1984. *Textbook of Polymer Science*. John Wiley and Sons; 3rd edition.

[2] Forum, W. E., 2016. *The New Plastics Economy — Rethinking the future of plastics*. Ellen Macarthur Foundation.

[3] Ogden, R. W., 1997. *Non-linear Elastic Deformations*. New York. Dover Publications.

[4] Suchocki, C., 2015. An internal-state variable based viscoelastic-plastic model for polymers. *Journal of Theoretical and Applied Mechanics*, vol. 53 (3), pp. 593–604.

[5] J.S. Bergström, M. B., 1998. Constitutive modeling of the large strain time-dependent behavior of elastomers. *J. Mech. Phys. Solids*, vol. 46, pp. 931–954.

[6] E.M. Arruda, M. B., 1993. A three-dimensional constitutive model for the large stretch behavior of rubber elastic materials. *IJ. Mech. Phys. Solids*, vol. 41 (2), pp. 389–412.

[7] J.S. Bergström, C.M. Rimnac, S. K., 2003. Prediction of multiaxial mechanical behavior for conventional and highly crosslinked uhmwpe using a hybrid constitutive model. biomaterials. vol. 24, pp. 1365–1380.

[8] A.D. Mulliken, M. B., 2005. Mechanics of the rate-dependent elastic–plastic deformation of glassy polymers from low to high strain rates. *International Journal of Solids ans Structures*, vol. 43, pp. 1331–1356.